DC Grid Control Through the Pilot Voltage Droop Concept

Mitigating consequences of time delays

Bertil Berggren, Ritwik Majumder
ABB Corporate Research
Västerås, Sweden
bertil.berggren@se.abb.com
ritwik.majumder@se.abb.com

Kerstin Lindén
ABB Power Systems
Ludvika, Sweden
kerstin.linden@se.abb.com

Abstract—**The control of the individual converters in a voltage-source-converter high-voltage dc (VSC-HVDC) based multi-terminal dc grid is central for the overall performance of the system. A few different variants of power drooped against dc voltage control have been proposed in the literature for the purpose of distributing the power mismatch, following a disturbance, on several converters. One such variant is the pilot voltage droop control concept which involves communication. As is always the case when communication is involved, there is a risk of latencies and even communication failure. This paper proposes a way to mitigate the consequences of latencies for the pilot voltage droop concept. The approach may also have bearing on other control problems, involving communication, where the aim is to adjust the steady state solution based on remote measurements. The proposed solution is established in a stepwise fashion starting from the basic control principle, and the performance is exemplified by time domain simulations with a four station dc grid using Digsilent's Powerfactory platform.**

Keywords— *High-voltage dc, voltage source converters, dc grid, droop control, time delays* .

I. INTRODUCTION

The possibility of introducing dc grids based on voltage-source-converter high-voltage dc (VSC-HVDC) transmission systems has during recent years received substantial interest [1]. One central aspect is the converter control and how to distribute a power mismatch following a disturbance on several converters in a predictable manner. This paper elaborates on a power drooped against direct voltage concept for the converter control in dc grids, the concept being referred to as the pilot voltage droop concept.

A number of droop control concepts have been proposed in the context of multi-terminal dc grid control in order to allow several converters to share a power mismatch following a disturbance. The proposed concepts typically rely on local measurements only. In, e.g., [2] the difference between power set-point and locally measured power is drooped against the difference between direct voltage set-point and measured local converter direct voltage. In [3] the difference between set-point in direct current and measured direct current output from the converter is drooped against the difference between global

(common for all converters) dc voltage set-point and local converter direct voltage. For the purpose of providing more degrees of freedom, [4] suggests different droop constants depending on the deviation between direct voltage set-point and measured value as a variation of [2]. Droop control concepts based on local voltage measurements suffer to some extent from the circumstance that the dc voltage magnitude varies across the dc grid due to resistance in the dc transmission. One way to reduce the influence of different local voltages is to compensate by adding a term consisting of injected current times a compensation constant (resistance) to the local voltage and by that control the voltage at a point beyond the converter terminal. For some small dc grids this has been a fruitful approach, as reported in e.g. [5] and [6], however for a more general grid structure it may be difficult to find good compensation constants to coordinate the voltage controls.

The pilot voltage droop concept uses communication for the purpose of establishing a common dc voltage signal across the dc grid. The objective is to achieve a performance similar to what is obtained for power drooped against frequency control in ac systems, where the common signal across the system is the frequency at steady state.

The pilot voltage droop concept was originally proposed in [7]. In [8] the concept was discussed in the context of adaptive droop. Reference [9] proposes different ways to re-establish set-point tracking for the approach if it has been lost due to both small and large disturbances. A power flow formulation for obtaining the post-disturbance steady state for a few different droop concepts, there among the pilot voltage droop concept, was suggested in [10]. In [11] a methodology for establishing fixed droop constants was outlined for the purpose of deciding the portion of a power mismatch that different converters should pick up following a disturbance such as e.g. a converter trip.

The main advantages with the pilot voltage droop concept are the precision with which a portion of a power mismatch can be directed to individual converters [11] and the straight forward fashion in which set-point tracking can be reestablished if it has been lost [9].

However, as the concept is based on communication, the consequences of time delays and even communication failure must be given attention. Time delays in feedback control are known to cause poor dynamic performance, limit cycles or even instability if not properly attended to.

The main contribution of this paper is a proposed approach for mitigating the consequences of latencies and even communication failure applicable to the pilot voltage droop concept.

The structure of the paper is as follows. Section II and III briefly describes the assumed station main circuit and the control system structure in which the pilot voltage droop control is introduced. Section IV describes the basic pilot voltage droop concept. The purpose of Section II - IV.A. is to establish the notation and assumed control framework. These sections are the same as in [9] and [11]. Section IV.B - IV.E which is the main contribution of this paper, describes the proposed approach for mitigating consequences of latencies in communication and communication failure. Conclusions are provided in Section V and the test system which has been used to illustrate the performance of the control is provided in the Appendix.

II. CONVERTER STATION MAIN CIRCUIT

Fig. 1 shows the main circuit of a converter station (of multi-level type). The following notation is used:

- P_{PCC}, Q_{PCC} : Active and reactive power at the point of common coupling (PCC).

- V_{PCC} : Voltage at PCC.

- I_v : Valve current.

- V_v : Valve voltage.

- V_{dc} : Converter direct voltage.

III. GENERAL CONVERTER CONTROL STRUCTURE

Fig. 2 illustrates the general converter control structure which will be assumed in this paper. The active power/direct voltage control block (AP/DV) takes as input, e.g., active power and direct voltage measurements together with set-points and generates a valve current order in d-axis direction as output. The reactive power/alternating voltage control block (RP/AV) takes as input, e.g., reactive power and alternating voltage measurements together with set-points and generates a valve current order in q-axis direction as output. The valve
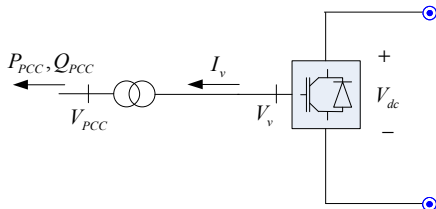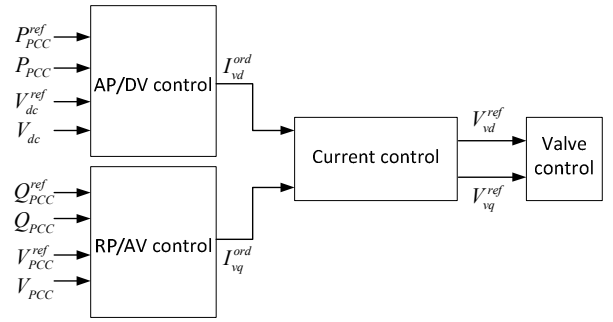

Fig. 2. General converter control structure.

current orders are fed into the valve current control block for the purpose of establishing valve voltage references which in turn are fed into the valve control block to be effectuated.

The general control structure, and specific example control implementations of each control block, can be found in [12], although similar proposals can be found elsewhere, see, e.g., [13] – [16].

The pilot voltage droop control, which is the focus of this paper, will be implemented by only changing the AP/DV control block as compared to [12] where a local voltage droop control was provided.

IV. PILOT VOLTAGE DROOP CONTROL

A. Basic Concept

An AP/DV control block for a basic pilot voltage droop control implementation is shown in Fig. 3. The feature that distinguishes the pilot voltage droop from other power drooped against dc voltage concepts is that all converters on this type of droop control receives the same dc voltage information. In other words, the pilot voltage error, $V_{dc,pilot}^{error}$, is common for all converters on pilot voltage droop control (for a bipole system it is common for all converters connected to the same pole network).

The pilot voltage measurement, $V_{dc,pilot}$, as such may be obtained as the dc converter voltage as measured at a specific point in the dc grid or it may be obtained as, e.g., the average of several converter voltages. It follows that the pilot voltage measurement, $V_{dc,pilot}$, and the corresponding set-point, $V_{dc,pilot}^{ref}$,

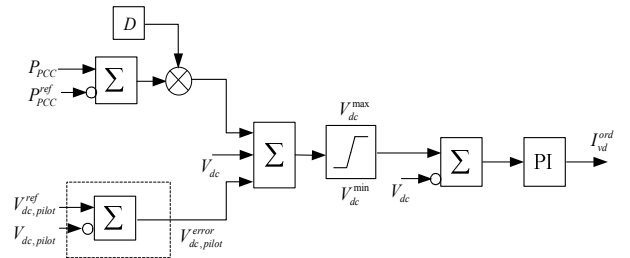

Fig. 1. Converter station main circuit.

Fig. 3. AP/DV control block for pilot voltage droop.

need to be communicated to all stations on this type of control.

The difference between measured active power at PCC, P_{PCC}, and the corresponding set-point, P_{PCC}^{ref}, is multiplied with a droop constant D.

It is here assumed that some sort of "dc grid code" will stipulate a dc voltage range within which the converters should operate, as also proposed in, e.g., [3]. By adding a measurement of the local dc voltage, V_{dc}, before a dc voltage limiter and then subtract it again after the limiter, the controls will not take the local dc voltage outside the allowed dc voltage range.

B. Establishing the Pilot Voltage Error

The basic pilot voltage droop control shown in Fig. 3 is useful for discussing the advantages it has in terms of distributing power mismatches according to droop constants in a precise manner, [11], and possibilities to establish set-point tracking, [9]. However in terms of dynamic performance it will not meet expected requirements for two reasons. The first problem is related to the circumstance that it tries to control a remote voltage, such that network dynamics between the converter and the remote measurement point may deteriorate the performance. The second problem is related to the risk of substantial transport delays in the communication between the point of measurement and the converter. In the following, it will be assumed that the remote measurements are received as sampled data with time stamps with global time reference (e.g. global positioning system (GPS) time, cf. phasor measurement unit (PMU) data time stamps). Furthermore, it is assumed that a clock with the same global time reference is available in the local control system. It is thus possible to determine the time delay of received data locally in the control system and switch over to a fallback control which is not dependent on communication in case excessive latencies are encountered. The purpose here is not to discuss pros and cons with various fallback strategies, several are conceivable, instead we select the one which is easiest to implement in this particular setting. Fig. 4 illustrates a more favorable way of establishing the pilot voltage error $V_{dc,pilot}^{error}$ as compared to the control in Fig. 3.

With the "fallback control" switch in the lower position, the droop control is only dependent on local measurements. This droop variant may be called power error drooped against local voltage error with a global voltage reference. This variant is similar to what is proposed in [3], although they use an error in direct current instead of active power error. This variant has good dynamic properties, but it lacks precision in terms of distributing a power mismatch according to the droop constants and set-point tracking cannot be established.
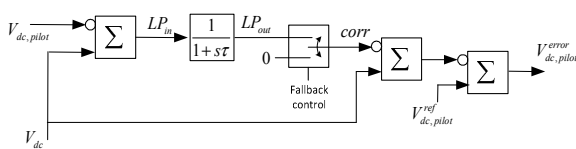
With the "fallback control" switch in the upper position, a low pass filtered correction term is added to the local voltage. We may write

$$V_{dc,pilot}^{error} = V_{dc,pilot}^{ref} - \left(V_{dc} - \frac{V_{dc} - V_{dc,pilot}}{1+s\tau} \right)$$

$$= \{\text{at steady state}\} = V_{dc,pilot}^{ref} - V_{dc,pilot}, \qquad (1)$$

i.e. in line with Fig. 3. Thus, in this way the pilot voltage droop control can be seen as power droop against local voltage error, but with a correction term. The purpose of the low pass filter is to improve the closed loop dynamic properties by removing the high frequency content in the correction term.

Fig. 5 shows an example of the input (blue) and output (red) of the low-pass filter with $\tau = 100\,[ms]$, i.e. with the cutoff frequency $f_c = 1.59\,[Hz]$. In this way, the control follows the fast dynamics in the local voltage, and the desired steady state is achieved by the addition of the more or less monotonically changing correction term.

As there is no intention of following the fast dynamics in the pilot voltage measurement, the requirement on sampling rate of the pilot voltage measurement is substantially reduced.

In order to illustrate the performance of the control, the test system outlined in the Appendix has been used. As a reference case a trip of positive pole converter in station 2 is considered. In Fig. 6 the active power at PCC in per unit is shown for both positive (blue) and negative (red) pole converters with low-pass filter, but without time delays. The trip of positive pole converter in station 2 (top right) occurs 3 s into the simulation and it can be seen that the positive pole power is adjusted for station 1 (top left), station 3 (lower left) and station 4 (lower right) on pilot voltage control, whereas the negative pole converters hardly are affected at all.
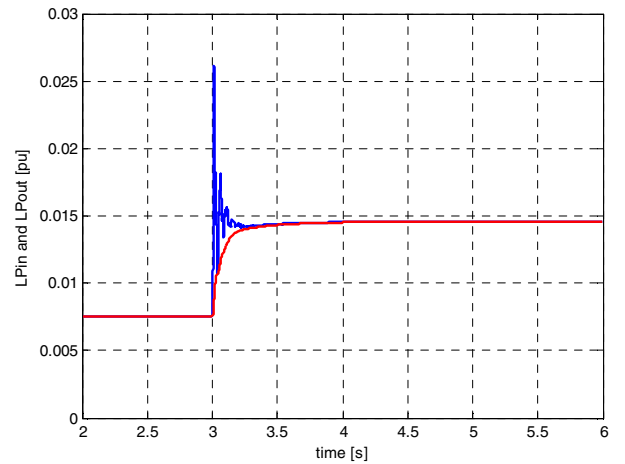

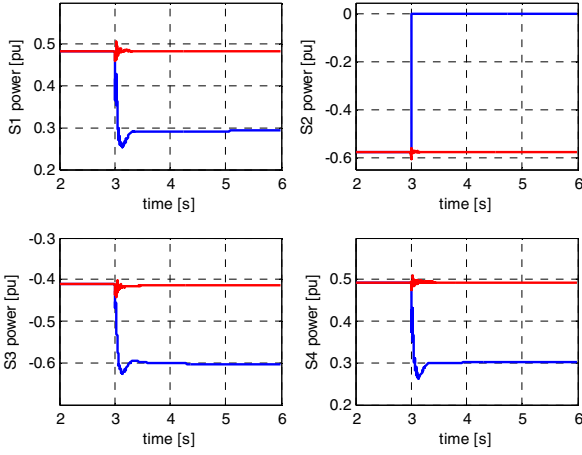Fig. 5. Example of low-pass filter input and output.

Fig. 4. Establishing the pilot voltage error.

Fig. 6. Active power – positive (blue) and negative (red) pole converters.

C. Introducing Time Delays

If transport delays, T_d, are introduced as indicated in Fig. 7 the behavior changes.

Fig. 8 shows the same case as in Fig. 6, but in this case with the time delays $T_{d1P} = T_{d1N} = 0.1\,[s]$, $T_{d3P} = T_{d3N} = 1\,[s]$, $T_{d4P} = T_{d4N} = 0.05\,[s]$. As can be seen the case is stable, but the dynamic performance is poor. Furthermore, it is quite easy to find combinations of time delays that yields an unacceptable
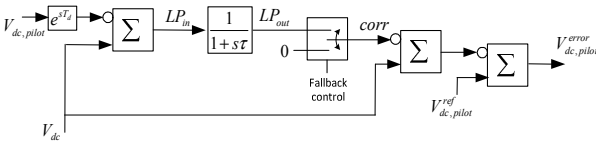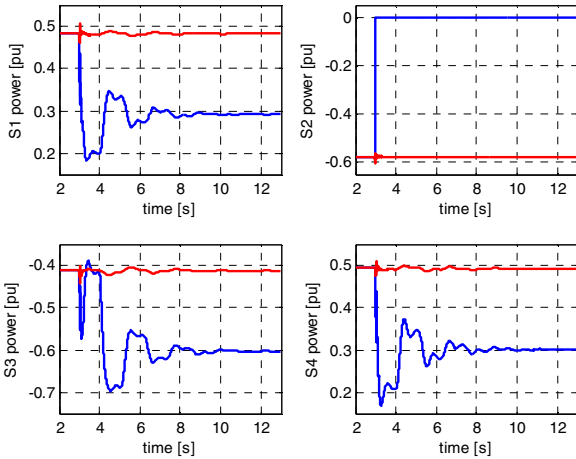

Fig. 7. Introducing transport delay.

Fig. 8. Active power with time delays.

behavior. For example, Fig. 9 shows the case when all delays instead are $T_d = 0.2\,[s]$.

The behavior suggests that a limit cycle (stable periodic attractor) has been obtained, i.e. the type of unfavorable behavior that is anticipated in systems with time delays in the feedback signal. The period of the oscillation is approximately 0.8 s, i.e. a frequency of approximately 1.25 Hz. This behavior not only involves the positive pole converters, but eventually also the negative pole converters locks to the oscillation.

$$V_{dc,pilot}^{error} = V_{dc,pilot}^{ref} - \left(V_{dc} - \frac{V_{dc} - e^{sT_d}V_{dc,pilot}}{1 + s\tau} \right) \qquad (2)$$

Having a look at how the pilot voltage error is obtained, (2), it can be seen that the separation of feedback signal into on one hand the local voltage with full dynamic content and on the other hand a low-passed filtered correction term has become blurred due to the delay. The local voltage with full dynamic content and the low-passed filtered local voltage approximately cancels out at the relatively low frequency of the standing oscillation, below the cutoff frequency of the low pass filter, leaving only a low-passed filtered time delayed pilot voltage in the feedback signal. This is of course the situation we would like to avoid. There might be possibilities to improve the situation by introducing some other type of low pass filter, however we will in the next section take another path to remedy the situation.

D. Intentional Delay of the Local Voltage

Recognizing that there really is no point in adjusting the correction term before information about the pilot voltage has arrived suggests that also the local voltage fed to the low-pass filter should be delayed.

In the control solution in Fig. 10, the local voltage that is fed to the low-pass filter is intentionally delayed, T_{dloc}, and if this delay is equal to the delay in the pilot voltage, the pilot voltage error can be written as
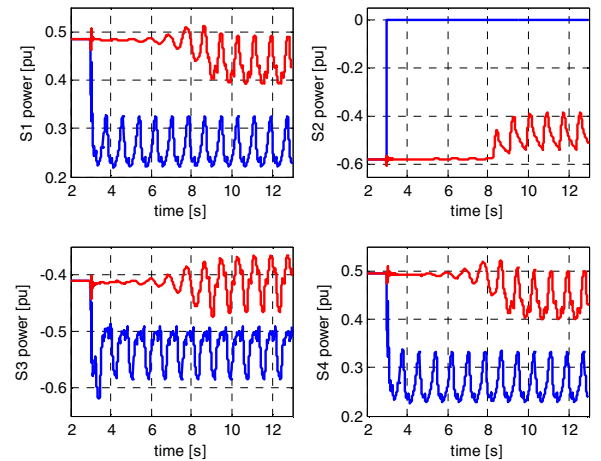

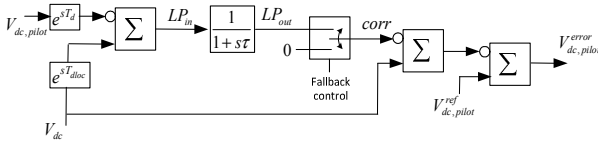Fig. 9. Active power with time delays.

Fig. 10. Intentional delay of local measurement.

$$V_{dc,pilot}^{error} = V_{dc,pilot}^{ref} - \left(V_{dc} - \frac{e^{sT_{dloc}} V_{dc} - e^{sT_d} V_{dc,pilot}}{1+s\tau} \right) =$$

$$= \{ T_{dloc} = T_d \} = V_{dc,pilot}^{ref} - \left(V_{dc} - e^{sT_d} \frac{V_{dc} - V_{dc,pilot}}{1+s\tau} \right). \quad (3)$$

Thus, in this case the separation of the feedback signal into the local voltage with full dynamic content and a low-passed filtered, although time delayed, correction term is maintained.

The size of the correction term is small as compared to the local voltage, in the same way as voltage drops between converters are small relative to the system voltage in a dc grid. In other words, the local voltage can be seen as the actual feedback signal whereas the correction term can be seen as a relatively small disturbance signal with low dynamic content.

In a real-time environment, the delay of the local voltage would probably be implemented by sampling the local voltage, time stamping it with global time reference and storing it. As pilot voltage measurements arrives, local voltage measurements with matching time stamps can be retrieved from storage (cf. data synchronization in a phasor data concentrator (PDC) unit).

The dynamic performance is substantially improved. Fig. 11 shows the response with intentional delay of the local voltage for the same case as shown in Fig. 9. As can be seen, there is no tendency to oscillatory behavior.

Fig. 12 shows the response for the same case as in Fig. 8, however in this case with intentional delay of the local voltage.
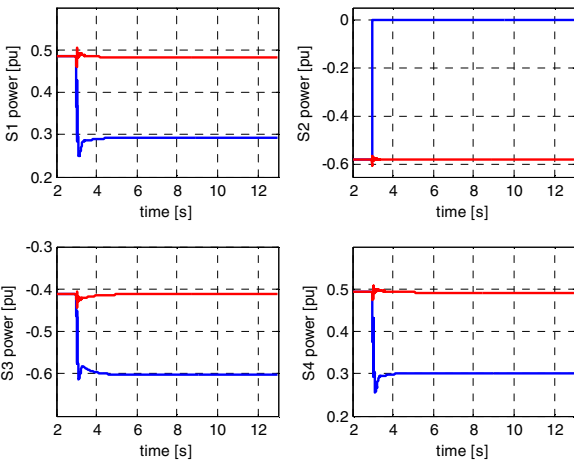

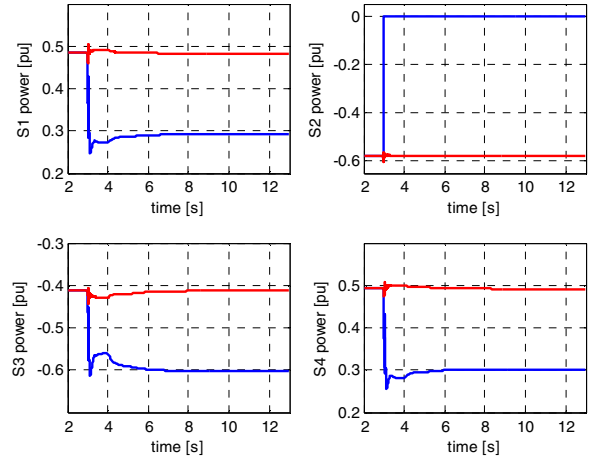Fig. 11. Active power with intentional local delay (cf. Fig. 9).

Fig. 12. Active power with intentional local delay (cf. Fig. 8).

As before, the trip occurs at 3 s, and in this case with a 1 s delay in station 3, the update of the correction term in station 3 can clearly be seen as a change in power in positive pole station 3 (lower left) at approximately 4 s, and that positive pole converters in station 1 (top left) and station 4 (lower right) adjusts to maintain power balance.

In the case shown in Fig. 13 the delays $T_{d1P} = T_{d1N} = T_{d4P} = T_{d4N} = 0.2\ [s]$, $T_{d3P} = T_{d3N} = 3\ [s]$, have been used, i.e. one delay is distinctly large.

Again, at 3 s the trip occurs and with a 3 s time delay a ringing effect can clearly be distinguished in positive pole station 3 power (lower left). Thus, at 6 s the correction term is updated with information from the disturbance, and similarly at 9 s the correction term is updated with the information from the update at 6 s and so on. The other converters adjusts their power to maintain power balance as a consequence of the updates of the correction term in positive pole station 3.

Thus, the dynamic performance is substantially improved, but there is of course no way to avoid that the convergence to
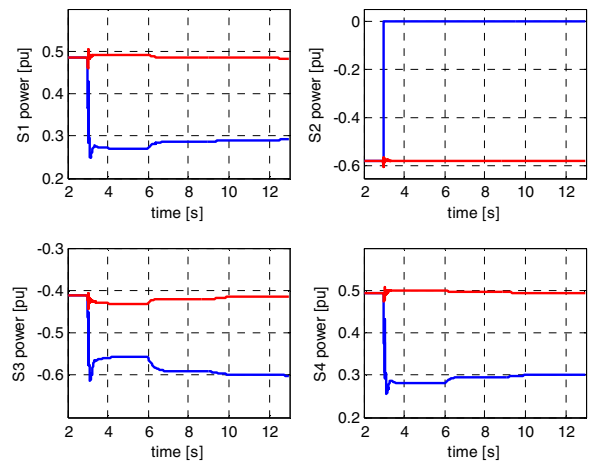

Fig. 13. Active power – one distinctly large delay.

steady state is somewhat slower as a consequence of the delays.

As there is no field experience available today, a clear indication of the size of the time delays to expect is unclear, however [17] reports time delays that normally were less than 30 ms, with occasional samples up to 200-300 ms, from a field test of a wide area power oscillation damping (WAPOD) application. Assuming similar performance of the communication in this application, time delays of in the order of a few hundred milliseconds would most likely not matter much as long as the dynamic performance is acceptable.

E. Communication Failure

With the intentional delay of local voltage as shown in Fig. 10, the consequences of a breakdown in communications are undramatic. The breakdown will locally be detected as a growing time delay in the pilot voltage. Neither pilot voltage samples nor local voltage samples will be fed to the low-pass filter and the correction term will simply freeze at what it was before the communication failed. When the time delay in a station exceeds a threshold, communication failure is inferred and switchover to fallback control may take place.

In Fig. 14, a case where communication with all stations fails at 2 s. At 3 s positive pole station 2 trips, and the droop control reacts to the disturbance although with frozen correction terms. When the time delays have reached a threshold of 8 s, i.e. 10 s into the simulation, switchover to fallback control occurs. Thus, the old and by this time inaccurate correction terms are removed for both positive and negative pole converters, and power error drooped against local voltage error with a global voltage reference is obtained, in this case for all stations.

Other fallback control strategies could of course be used, and obviously, only stations experiencing excessive time delays (communication failures) need to switchover to fallback control.
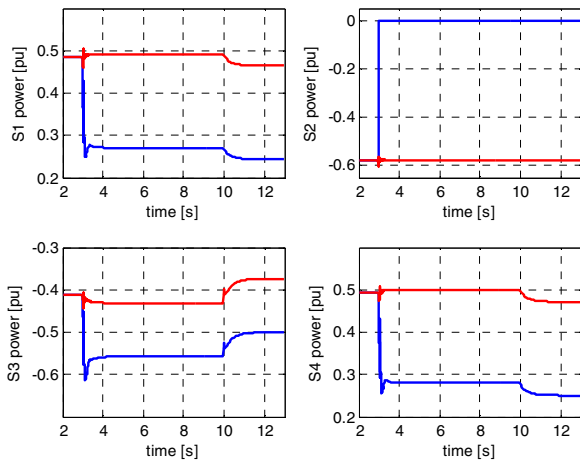

Fig. 14. Active power – communication failure.

V. CONCLUSIONS

In this paper, a concept for mitigating consequences of time delays in communication is proposed for the pilot voltage droop concept. Instead of directly using the remote pilot voltage measurement signal, which may be exposed to latencies, the basic idea is to divide this feedback signal into on one hand the local voltage with full dynamic content plus on the other hand a correction term. At steady state the sum of the two parts is equal to the pilot voltage signal. The correction term is low-pass filtered and the local voltage which also constitutes a part of the correction term is intentionally delayed to improve the dynamic performance of the control.

This concept for handling time delays has shown good and robust dynamic performance in our studies. The circumstance that delayed measurement samples also delays convergence to steady state at a disturbance is however something that is unavoidable with this concept. However, as long as the delays are within limits, this should not have any consequences in practice. If the delays are considered too long switchover to fallback control based on local measurements may be performed.

This concept for handling time delays has the potential of being useful also for other applications where the aim is to adjust the steady state based on remote measurements.

VI. APPENDIX

As an example the same small test system as in e.g. [9] and [10] has been implemented together with the controls in a commercially available software platform, namely PowerFactory provided by the company Digsilent. Some hints on how to implement the controls on this platform can be found in [12].

In the four station dc grid, Fig. 15, with bipole structure, the four stations are interconnected with four sets of cables. Each of the cable sets consists of positive pole, negative pole and metallic return cables. The neutral point system, to which the metallic return cables are connected, is directly grounded at station 1. The ac system is represented with one ac voltage source connected to each station PCC. The converter model in PowerFactory is an average model with positive sequence phasor representation on the ac side and instantaneous value representation on the dc side. The 320 kV cables are represented with lumped parameters (π), where $r = 0.0146\left[\Omega / km\right], l = 0.1463\left[mH / km\right], c = 0.2662\left[\mu F / km\right]$ and all cables are 400 km. Each pole converter is rated 608 MVA and the nominal direct voltage is 320 kV (pole-to-ground).

Station 1, 3 and 4 are configured to be on pilot voltage droop control, whereas station 2 is assumed to be connected to a wind farm which for the purpose of this test system is represented as a constant power controlled station. The
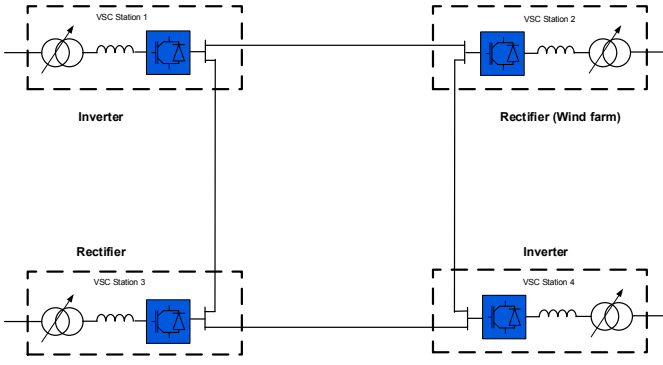
Fig. 15. Four station dc system.

converter voltages (positive and negative pole respectively) of station 4 are used as pilot voltage measurements.

The pre-disturbance operating point is shown in Table I where $P_{PCC,p}$ and $P_{PCC,n}$ are the power in MW at PCC for positive and negative pole respectively (positive power corresponds to inverter operation). V_p, V_n and V_m are the positive pole to ground, negative pole to ground and mid-point to ground direct voltages in kV respectively. It can be concluded that the pre-disturbance steady state corresponds to symmetric operation with 5.74 MW losses per pole. The power and pilot voltage deviations at pre-disturbance steady state are assumed to be zero, i.e., the power schedule is established. In other words, the power references are equal to actual power in column 2 and 3 in Table I and the pilot voltages references are obtained as

$$V_{dc,pilot,p}^{ref} = 303.94 - 0.0 = 303.94 \left[kV \right],$$
$$V_{dc,pilot,n}^{ref} = 0.0 - -303.94 = 303.94 \left[kV \right], \tag{4}$$

based on the voltages at station 4.

All droop constants are assumed equal in this case, namely $D_{1p} = D_{3p} = D_{4p} = 0.04 \left[kV / MW \right]$, and similar for the negative pole. Table II provides parameters used in the simulations.

TABLE I. PRE-DISTURBANCE OPERATING POINT.

Station	$P_{PCC,p}$	$P_{PCC,n}$	V_p	V_n	V_m
1	+294.26	+294.26	303.99	-303.99	0.00
2	-350.00	-350.00	307.29	-307.29	0.00
3	-250.00	-250.00	306.35	-306.35	0.00
4	+300.00	+300.00	303.94	-303.94	0.00

TABLE II. PARAMETERS USED IN SIMULATIONS.

Variable	Value	Description
SCC	43648 MVA	Short circuit capacity of strong ac network
V_{Bac}	208 kV	Converter ac voltage base
V_{Bdc}	320 kV	DC voltage base
S_B	608 MVA	Converter MVA
K_{P1}	2.8	Proportional gain (AP/DV control)
K_{I1}	41	Integral gain (AP/DV control)
D	0.04kV/MW	Droop constant
τ	100 ms	Low-pass filter time constant
A_Q	1	RP control
A_V	0	RP control
K_{P2}	0.4	Proportional gain (RP/AV control)
K_{I2}	70	Integral gain (RP/AV control)
K_{PI}	0.4743	Proportional gain (current control)
k_p	15	PLL proportional gain
k_i	20	PLL integral gain
X_r	0.06004 pu	Equivalent phase reactor

REFERENCES

[1] CIGRE WG B4.52, 'Feasibility of HVDC grids,' CIGRE technical brochure 533, Paris, April 2013.

[2] T.M. Haileselassie, K. Uhlen, 'Primary Frequency Control of Remote Grids Connected by Multi-terminal HVDC,' IEEE Power and Energy Society General Meeting, vol., no., pp.1-6, 25-29 July 2010.

[3] C.D. Barker, R. Whitehouse, 'Autonomous Converter Control in a Multi-Terminal HVDC System,' in Proc. 9th IET Int. Conf. ACDC Power Transmission, vol., no., pp. 1-5, 19-21 Oct. 2010.

[4] T.K. Vrana, L. Zeni, O.B. Fosso, 'Active Power Control with Undead-band Voltage & Frequency Droop for HVDC Converters in Large Meshed DC Grids,' EWEA Conference, Copenhagen, April 2012.

[5] X. Lie, B.W. Williams, Y. Liangzhong, 'Multi-Terminal DC Transmission Systems for Connecting Large Offshore Wind Farms,' IEEE Power and Energy Society General Meeting - Conversion and Delivery of Electrical Energy in the 21st Century, vol., no., pp.1-7, 20-24 July 2008.

[6] J. Liang, O. Gomis-Bellmunt, J. Ekanayake, N. Jenkins, 'Control of multi-terminal VSC-HVDC transmission for offshore wind power,' Power Electronics and Applications, 2009. EPE '09. 13th European Conference on , vol., no., pp.1-10, 8-10 Sept. 2009.

[7] B. Berggren, R. Majumder, C. Sao, K. Linden, 'Method and Control Device for Controlling Power Flow within a dc Power Transmission Network,'WIPO International Publication Number WO 2012/000549 A1, International Filing Date: 30 June 2019; International Publication Date: 5 January 2012.

[8] N.R. Chaudhuri, B. Chaudhuri, 'Adaptive Droop Control for Effective Power Sharing in Multi-Terminal DC (MTDC) Grids,' IEEE Transactions on Power Systems, vol.28, no.1, pp.21-29, Feb. 2013.

[9] Berggren, B.; Linden, K.; Majumder, R., 'DC grid control through the pilot voltage droop concept - Methods for establishing set-point tracking,' Energy Conference (ENERGYCON), 2014 IEEE International, vol., no., pp.1562,1569, 13-16 May 2014.

[10] Berggren, B.; Linden, K.; Majumder, R., 'On static contingency analysis for combined HVAC and VSC HVDC grids,' CIGRE Belgium Conference, 12-14 March 2014.

[11] Berggren, B.; Linden, K.; Majumder, R., 'DC grid control through the pilot voltage droop concept – Methodology for Establishing Droop Constants,' IEEE Transactions on Power Systems, in press.

[12] B. Berggren, R. Majumder, N. Johansson, 'A Generic VSC HVDC Primary Control Structure Suitable for Stability Studies,' 2013 EPRI HVDC & FACTS Conference, pp. 1-8, Palo Alto, USA, 28-29 Aug. 2013.

[13] J. Peralta, H. Saad, S. Dennetiere, J. Mahseredjian, 'Dynamic performance of average-value models for multi-terminal VSC-HVDC systems,' IEEE Power and Energy Society General Meeting, vol., no., pp.1-8, 22-26 July 2012.

[14] A.M. Alsseid, D. Jovcic, A. Starkey, 'Small signal modelling and stability analysis of multiterminal VSC-HVDC,' Proceedings of the 2011-14th European Conference on Power Electronics and Applications, vol., no., pp.1-10, Aug. 30 -Sept. 1, 2011.

[15] B. Jacobsson, P. Karlsson, G. Asplund, L. Harnefors and T. Jonsson, 'VSC-HVDC Transmission with Cascaded Two-Level Converters,' CIGRE Session, pp. B4-B110, 2010.

[16] T.M. Haileselassie, M. Molinas and T. Undeland, "Multi-Terminal VSC-HVDC System for Integration of Offshore Wind Farms and Green Electrification of Platforms in North Sea", Nordic Workshop on Power and Industrial Electronics, June 9-11, 2008.

[17] K. Uhlen, L. Vanfretti, M.M. de Oliveira, A.B. Leirbukt, V.H. Aarstrand, J.O. Gjerde, "Wide-Area Power Oscillation Damper Implementation and Testing in the Norwegian Transmission Network," Power and Energy Society General Meeting, 2012 IEEE, vol., no., pp.1,7, 22-26 July 2012.